The Azimuthal Distribution of Dust Particles in an Eccentric Protoplanetary Disk with an Embedded Gas Giant Planet

Pin-Gao Gu and He-Feng Hsieh

Instituter of Astronomy & Astrophysics, Academia Sinica,
Taipei 10617, Taiwan
email: gu@asiaa.sinica.edu.tw

Abstract. We investigate the dust velocity and spatial distribution in an eccentric protoplanetary disk under the secular gravitational perturbation of an embedded planet of about 5 Jupiter masses. We first employ the FARGO code to obtain the two-dimensional density and velocity profiles of the gas disk with the embedded planet in the quasi-steady state. We then apply the secular perturbation theory and incorporate the gas drag to estimate the dust velocity on the secular timescale. The dust-to-gas ratio of the unperturbed disk is simply assumed to be 0.01. In our fiducial disk model with the planet at 5 AU, we find that for 0.01 cm– to 1 m–sized dust particles well coupled to the gas, the dust behaves similarly to the gas and exhibits non-axisymmetric dynamics as a result of eccentric orbits. However, for the case of a low-density gaseous disk (termed "transition disk" henceforth in this article) harboring the planet at 100 AU, the azimuthal distributions of dust of various sizes can deviate significantly.

Keywords. celestial mechanics, hydrodynamics, planetary systems: protoplanetary disks

---

1. Introduction

The presence of a cavity and/or non-axisymmetric features in a protoplanetary disk as revealed by dust continuum emissions has at times been postulated as a potential signpost of an embedded gas giant planet (Andrews *et al.* 2011). If the planet is sufficiently massive, the disk exterior to the planet's orbit can become moderately eccentric and start precessing on the secular timescale, depending on the disk mass and viscosity (Dunhill *et al.* 2012). In such an eccentric protoplanetary disk harboring a massive planet, the orbits of dust particles would be eccentric as well due to the gas drag.

We run the FARGO code (Masset 2000) to obtain the gas profile in a two-dimensional disk with a massive planet, and then employ the secular perturbation theory and incorporate aerodynamic drag (Paardekooper *et al.* 2008) to estimate the dust velocity and density that will in turn reveal the asymmetric structures inherent to an eccentric disk. The purpose of this study is to focus only on the secular behaviors of dust associated with an eccentric protoplanetary disk in the presence of a massive giant planet. Therefore, non-secular effects, such as dust-gas dynamics in the horseshoe orbit and whether dust particles can drift toward the peaks of spiral density waves in an eccentric disk (e.g., Fouchet *et al.* 2010), are not studied in this work.

2. Approach

We adopt the standard disk parameters for our fiducial model (Kley & Dirksen 2006): stellar mass = $1 M_\odot$, planet mass = $5 M_{jup}$, disk aspect ratio $H/r = 0.05$ (i.e., locally

isothermal), planet location $= a_p = 5$ AU for a protoplantary disk and 100 AU for a transition disk, kinematic viscosity $\nu = 10^{-5} a_p^2 \Omega_p$, surface density $\Sigma = 10^{-4} M_\odot / a_p^2$, planet eccentricity is zero, and dust-to-gas ratio in the basic state is 0.01. The gas information in a steady state is obtained from the 2D disk simulation using the FARGO.

To reveal secular features associated with eccentric disks, we average the gas disk properties over one orbital period of the planet. After obtaining the secular properties of the disk gas, we employ the secular perturbation theory of dust with the gas drag to calculate the dust surface density and velocities (Paardekooper *et al.* 2008).

The steady state in the secular perturbation theory is considered; namely, the gas drag is balanced by planet's potential. We define the "secular" dimensionless stopping time $\tau_{s,sec} \equiv t_{stop}/t_{precession}$, where t_{stop} is the stopping time in the Epstein regime (Weidenschilling 1977) and $t_{precession}$ is the precession time of a particle due to the planet's potential. If $\tau_{s,sec} \ll 1$, the dust is well coupled to the gas on the secular timescale. On the other hand, if $\tau_{s,sec} \approx 1$, the dust is then weakly coupled to the gas on the secular timescale.

3. Results

Fig. 1 shows the azimuthally averaged eccentricities of the gas and dust of various sized in the cases of the protoplanetary (left panel) and transition disks (right panel). In the case of of the protoplanetary disk, all the curves overlap in the region $r > 2$. It is because $\tau_{s,sec} \ll 1$. In contrast, the eccentricity profile for 1 m particles are rather small in the transition disk. It arises because 1 m particles become weakly coupled to the gas (i.e., $\tau_{s,sec} \approx 1$) in the low gas density environment of the transition disk. Hereafter, we focus only on the velocity and density profiles almost exterior to the gap (i.e., $r > 2$) where the disks become eccentric. The radial velocities associated with the eccentric orbits are computed. We find that they can reach 745 m/s in the region around the gap in the protoplanetary disk. In the transition disk, while the radial velocities are only $\leqslant$ 40-50 m/s for 1 m particles, they can be as high as 170 m/s for smaller particles.

Fig. 2 shows a snapshot of the spatial distribution of the dust surface density for 0.01 cm and 1 m particles in both the protoplanetary and transition disks. The distributions exhibit $m = 1$ structures with the density excess about 5-10% around the apocenter. The dust enhancement is caused by the gas streamlines converge near the apocenter of the disk. All the $m = 1$ dust distributions look quite similar except for that for the 1 m particles in the transition disk shown in the lower bottom panel. For those large particles in the transition disk, $\tau_{s,sec} \approx$ 1-10 and thus the particles are weakly coupled. As a result, the 1 m particles precess with the gas disk but with a phase lag $\approx \arctan \tau_{s,sec} \approx 80°$, as illustrated in Fig. 2.

4. Summary

The most important parameter for determining the gas-dust coupling on the secular timescales in an eccentric disk is $\tau_{s,sec}$, the secular stopping time defined as the ratio of the stopping time to the precession timescale for a free particle. The short-period features, such as the tightly wound density waves, probably present formidable challenges to be observationally resolved, but the secular features presented in this poster are more large-scale, comparable to the gap size, and thus more promising detection-wise. There exists a phase correlation for the $m = 1$ structure between the gas velocity fields and dust density distribution in an eccentric disk with an embedded massive planet. The velocity departure from the Keplerian circular motion in our model can be larger than 150 m/s,
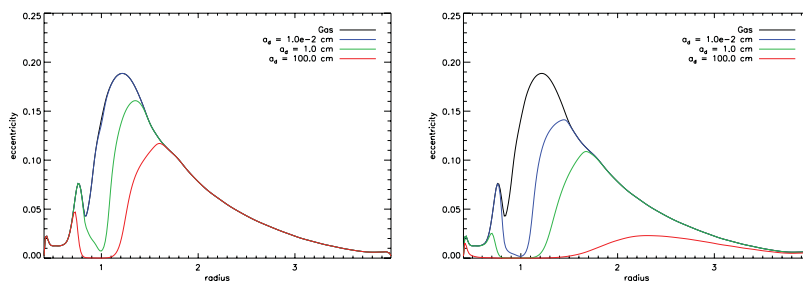
Figure 1. Azimuthal averaged eccentricities of the gas and dust of various sizes in the cases of the protoplanetary (left panel) and transition (right panel) disks. The planet is located at the radius $r = 1$.
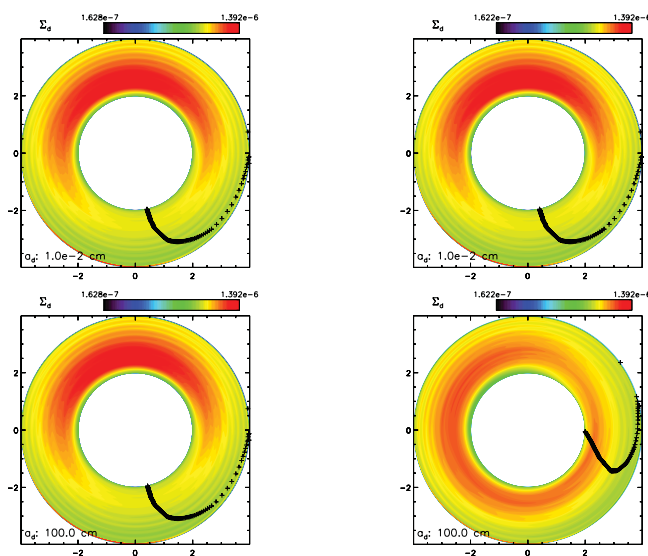
Figure 2. Spatial distribution of the dust surface density for 0.01 cm and 1 m particles in the cases of the protoplanetary (left panels) and transition disks (right panels). The units of the surface density are about 0.356 g/cm^2 and 9×10^{-4} g/cm^2 for the protoplanetary and transition disks, respectively. The plus signs in the plot mark the azimuthally averaged longitude of pericenter of particles.

which is probably high enough for ALMA detectability. In addition, the maximum dust emissions should be aligned with the apocenter of the eccentric gap in an eccentric disk. We show that particles of sizes of 1 m and 1 cm may be distributed differently in the azimuthal direction of an eccentric disk with a low gas density. This phenomenon may be revealed by measuring the spectral energy distribution with EVLA in different azimuthal directions covering the wavelengths from 1 to tens of cm. This work is partly supported by the NSC grant in Taiwan through NSC 100-2112-M-001-005-MY3.

References

Andrews, S. M. *et al.* 2011, *ApJ*, 732, 42
Dunhill, A., Alexander, R., & Armitage, P. 2012, *MNRAS*, 428, 3072

Fouchet, L., Gonzalez, J.-F., & Maddison, S. T. 2010, *A&A*, 518, 16
Kley, W. & Dirksen, G. 2006, *A&A*, 447, 369
Masset, F. 2000, *A&AS*, 141, 165
Paardekooper, S.-J., Thébault, P., & Mellema, G. 2008, *MNRAS*, 386, 973
Weidenschilling, S. J. 1977, *MNRAS*, 180, 57